

# Förster Resonance Energy Transfer Study of Cytochrome *c*—Lipid Interactions

Galyna P. Gorbenko<sup>1</sup> · Valeriya Trusova<sup>1</sup> · Julian G. Molotkovsky<sup>2</sup>

Received: 14 July 2017 / Accepted: 30 August 2017 / Published online: 6 September 2017  
© Springer Science+Business Media, LLC 2017

**Abstract** Specific interactions between a mitochondrial hemoprotein cytochrome *c* (cyt *c*) and cardiolipin, a lipid component of mitochondrial membrane, are crucial to electron shuttling and apoptotic activities of this protein. In the present study the Förster resonance energy transfer (FRET) between anthrylvinyl-labeled phosphatidylcholine as a donor and heme moiety of cyt *c* as an acceptor was employed to give a quantitative characterization of the protein binding to the model membranes from the mixtures of phosphatidylcholine (PC) with phosphatidylglycerol (PG), phosphatidylserine (PS) or cardiolipin (CL) in different molar ratios. The multiple arrays of the FRET data were globally analyzed in terms of the model of energy transfer in two-dimensional systems combined with the scaled particle adsorption model. The arguments in favor of the specificity of cyt *c* interactions with CL were obtained, including the higher adsorption potential and the deeper protein insertion in the lipid bilayer.

**Keywords** Cytochrome *c* · Cardiolipin · Protein-lipid interactions · Förster resonance energy transfer

## Introduction

The Förster resonance energy transfer (FRET) has long been recognized as one of the most powerful fluorescence

techniques capable of providing both qualitative and quantitative information on a diversity of processes occurring in biological membranes [1–4]. This technique proved to be particularly efficient in elucidating the nature of interactions between the protein and lipid membrane components [5]. FRET has been employed to gain insight into protein adsorption on a lipid bilayer [6], proximity relationships in the protein-lipid complexes [7], lipid domain formation [8], protein conformational changes in a membrane environment [9, 10], lipid-mediated protein aggregation and fibril formation [11, 12], etc. A great deal of the FRET membrane studies are carried out with the model protein-lipid systems composed of lipid vesicles of a given composition and isolated proteins. There are different formats of FRET measurements in which donors and acceptors may be intrinsic protein fluorophores, covalent protein or lipid labels, and fluorescent dyes non-covalently associating with proteins or lipids. One of these formats involves the case when the energy acceptors pertaining to the water-soluble protein distribute between the aqueous and lipid phases, while the donors are embedded in a lipid bilayer at a known depth through covalent labeling of lipid molecules in a certain position. In this case the efficiency of energy transfer depends both on transverse location of the protein molecule in a lipid bilayer and the acceptor surface concentration, which, in turn, is determined by the extent of the protein-membrane binding. Thus, in principle, it is possible to extract both structural (the depth of the protein insertion in the lipid bilayer) and binding (association constant and binding stoichiometry) parameters from the FRET measurements. As we demonstrated previously, the global analysis of two-dimensional array of FRET data acquired by varying both protein and lipid concentrations allows to circumvent the problem of parameter cross-correlation and determine both structural and binding characteristics of the protein-lipid complexes with high accuracy and statistical significance [13]. In the present work this approach was

✉ Galyna P. Gorbenko  
galyna.p.gorbenko@karazin.ua

<sup>1</sup> Department of Nuclear and Medical Physics, V.N. Karazin Kharkiv National University, 4 Svobody Sq., Kharkiv 61022, Ukraine

<sup>2</sup> Shemyakin-Ovchinnikov Institute of Bioorganic Chemistry, Russian Academy of Sciences, 16/10 Miklukho-Maklaya Str., Moscow 117997, Russia

employed to gain further insights into lipid bilayer interactions of cytochrome *c*.

Cytochrome *c* (cyt *c*), a highly basic hemoprotein found in the intermembrane space of mitochondria, plays an essential role in the two extensively studied physiological processes – electron transfer in the respiratory chain of the inner mitochondrial membrane and programmed cell death, apoptosis [14–16]. Both these processes are thought to be mediated by cyt *c* interaction with cardiolipin (CL), an anionic mitochondrial glycerophospholipid with unique physicochemical properties [17]. The molecular mechanisms of cyt *c* binding to CL have long been a focus of considerable research efforts, shedding light on a variety of important aspects of this problem [18–20]. The current consensus points to a multistep character of cyt *c* – CL complexation that may be divided into at least three interdependent stages: (i) the protein adsorption at the lipid-water interface initially driven by electrostatic forces and then followed by hydrogen bonding and hydrophobic interactions [21–23]; (ii) CL-induced conformational changes of cyt *c* involving varying degrees of the protein unfolding and opening of the heme crevice [24–26]; (iii) structural transformations of the lipid bilayer associated with CL clustering and the formation of lipid phases with negative curvature [27–29].

However, notwithstanding considerable advances in molecular-level understanding of cyt *c*-CL interactions, the precise mechanisms of this process still remain to be fully elucidated. One of the unresolved questions is how specific features of CL distinguishing it from other anionic phospholipids operate in determining the structural and functional peculiarities of cyt *c*-CL complexes. While addressing this issue in the present study, we employed the Förster resonance energy transfer to compare the lipid-associating characteristics of cyt *c* in the model protein-lipid systems containing as a lipid component lipid vesicles from phosphatidylcholine and varying proportions of one of the anionic phospholipids, cardiolipin, phosphatidylglycerol (PG) or phosphatidylserine (PS). To this end, the following objectives were pursued: (i) to explore the binding of cyt *c* to lipid bilayers by measuring the efficiency of energy transfer between anthrylvinyl-labeled PC (AV-PC) as a donor and heme group of the protein as an acceptor; (ii) to estimate the binding and structural parameters for cyt *c*-lipid complexes through the global analysis of the experimental data in terms of the combined adsorption-FRET model.

## Materials and Methods

### Chemicals

Bovine heart cardiolipin and horse heart cyt *c* (oxidized form) were purchased from Sigma (St. Louis, MO, USA).

1-palmitoyl-2-oleoyl-sn-glycero-3-phosphocholine (PC) and 1-palmitoyl-2-oleoyl-sn-glycero-3-phospho-rac-glycerol (PG), 1-palmitoyl-2-oleoyl-sn-glycero-3-phospho-L-serine (PS) were from Avanti Polar Lipids (Alabaster, AL). Fluorescent lipid, (1-acyl-2-[12-(9-anthryl)-11-trans-dodecenoyl]-sn-glycerophosphocholine, 1-acyl: 16:0/18:0 = 3/1) was synthesized as described in detail elsewhere [30, 31]. All other chemicals were of analytical grade and used without further purification.

### Preparation of Lipid Vesicles

Large unilamellar vesicles were prepared by extrusion technique from PC mixture with PG (10, 20 and 40 mol %), PS (10, 20 and 40 mol %) or CL (5, 11 and 25 mol% CL). Appropriate amounts of lipid stock solutions were mixed in chloroform, evaporated to dryness under a gentle nitrogen stream, and then left under reduced pressure for 1.5 h to remove any residual solvent. The dry lipid residues were subsequently hydrated with 5 mM sodium-phosphate buffer, pH 7.4 at room temperature to yield lipid concentration of 1 mM. Thereafter, the sample was subjected to 15 passes through a 100 nm pore size polycarbonate filter (Millipore, Bedford, USA), yielding the liposomes of desired composition. AV-PC (0.3 mol % of total lipid) was added to the lipid mixture prior to the solvent evaporation. The concentration of fluorescent lipid was determined spectrophotometrically using the anthrylvinyl extinction coefficient  $\epsilon_{367} = 9 \times 10^3 \text{ M}^{-1} \text{ cm}^{-1}$  (in ethanol) [31]. Hereafter, the liposomes containing 10, 20 or 40 mol% PG (PS) are referred to as PG10, PG20, PG40 (PS10, PS20, PS40), while the liposomes containing 5, 11 or 25 mol% CL are referred to as CL5, CL11, CL25, respectively.

### Fluorescence Measurements

Fluorescence measurements were performed at 25 °C with LS-50 spectrofluorimeter (Perkin-Elmer Ltd., Beaconsfield, UK) using 10-mm path-length quartz cuvettes. AV-PC emission spectra were recorded with 367 nm excitation. Excitation and emission bandpasses were set at 5 nm. The FRET experiments were conducted with AV-PC as a donor and heme group of cyt *c* as an acceptor. Fluorescence intensity measured in the presence of cyt *c* at the maximum of AV emission (434 nm) was corrected for the reabsorption and inner filter effects using the following coefficients [32]:

$$k = \frac{(1 - 10^{-A_o^{ex}})(A_o^{ex} + A_a^{ex})(1 - 10^{-A_o^{em}})(A_o^{em} + A_a^{em})}{(1 - 10^{-(A_o^{ex} + A_a^{ex})})A_o^{ex}(1 - 10^{-(A_o^{em} + A_a^{em})})A_o^{em}} \quad (1)$$

where  $A_o^{ex}$ ,  $A_o^{em}$  are the donor optical densities at the excitation and emission wavelengths in the absence of acceptor,

$A_a^{ex}$ ,  $A_a^{em}$  are the acceptor optical densities at the excitation and emission wavelengths, respectively. The relative quantum yield of the donor ( $Q_r$ ) was determined by measuring the decrease of AV fluorescence upon addition of cyt *c*:

$$Q_r = \frac{Q_{DA}}{Q_D} \tag{2}$$

where  $Q_D$ ,  $Q_{DA}$  are the donor quantum yields in the absence and presence of acceptor, respectively. The steady-state fluorescence anisotropy of AV fluorophore was measured at the excitation and emission wavelengths of 367 and 434 nm, respectively, with excitation and emission bandpasses set at 10 nm.

## Results and Discussion

### Comparative Qualitative Analysis of FRET Between AV-PC and Heme Group of cyt *c* in PC/CL, PC/PS and PC/PG Model Membranes

The Förster resonance energy transfer from AV-PC to the heme group of cyt *c* was explored by monitoring the decrease of the donor fluorescence upon addition of the acceptor. The FRET experiments were designed to acquire the multiple data arrays required for the proper quantification of the obtained results. The relative quantum yield of AV-PC was measured as a function of the following variables: i) the total protein concentration ( $P$ ), 12 points taken from the range 0.02–0.54  $\mu\text{M}$ ; ii) the total lipid concentration ( $L$ ), 4 points, from the range 5–40  $\mu\text{M}$ ; iii) the molar fraction of anionic phospholipid (0.1, 0.2, 0.4 for PG and PS; 0.05, 0.11, 0.25 for CL). In Figs. 1, 2, and 3 the relative quantum yield of AV-PC is plotted as a function of the protein and lipid concentration for different types of liposomes. One of the conspicuous features of the presented FRET profiles is that the most effective energy transfer occurs in the CL-containing systems. This finding cannot be explained by the higher surface electrostatic potential of PC/CL bilayers, because the molar proportion of CL was chosen to ensure the values of this parameter similar to those of PC/PG or PC/PS bilayers. Although the degree of CL protonation has long been a matter of controversy, recent study of Malyshka et al. provided convincing evidence that CL is fully deprotonated at neutral pH, bearing the charge  $-2e$  [33]. Accordingly, the surface electrostatic potential calculated in terms of the Gouy-Chapman double layer theory for protein-free lipid vesicles possess the values  $\{-90, -126, -162\}$  mV for  $\{\text{CL5}, \text{CL11}, \text{CL25}\}$  liposomes, and  $\{-92, -126, -161\}$  mV for  $\{\text{PG(PS)10}, \text{PG(PS)20}, \text{PG(PS)40}\}$  liposomes, respectively.

Also worthy of mention is the fact that the most pronounced differences between the FRET curves measured for the liposomes with similar surface charge are observed at the lowest content of anionic lipids (Fig. 1). This presumably arises from the distinctions between the different types of lipid vesicles in the extent of the protein binding and the heme position with respect to the lipid bilayer surface. The relative quantum yield of the donor ( $Q_r$ ) is determined by the two main parameters: the amount of the membrane-bound acceptors that is equal to the concentration of bound protein ( $B$ ) and the distance of the heme group from the bilayer midplane ( $d_c$ ). In turn, the concentration of the membrane-adsorbed protein is a function of the association constant ( $K_a$ ) and the number of lipids per bound protein ( $n$ ). Thus, the experimental  $Q_r(P)$  profiles depend on  $d_c$  value and actually reflect the behavior of  $B(P)$  curves. Evidently, in the case of complete protein-membrane binding  $d_c$  becomes the only parameter determining the differences between the obtained FRET profiles. To describe these differences in quantitative terms, we employed the theoretical approach combining the adsorption and FRET models purposefully developed for the protein-lipid systems.

### Quantification of the Energy Transfer Profiles in Terms of the Combined Adsorption-FRET Model

The association of cyt *c* with the model lipid membranes was analyzed in terms of the scaled particle adsorption model which adequately describes the excluded area interactions between the adsorbing protein molecules [34, 35]. In terms of this model the activity coefficient of the adsorbed spherical ligand is given by:

$$\gamma = \frac{1}{1-\theta} \exp\left(\frac{3\theta}{1-\theta} + \left[\frac{\theta}{1-\theta}\right]^2\right); \theta = nB/L_{out} \tag{3}$$

where  $\theta$  is the fraction of surface area occupied by the adsorbed protein;  $B$  is the concentration of the bound species;  $n$  stands for the number of lipids per molecule of the adsorbed protein;  $L_{out}$  is the concentration of accessible lipids related to the total lipid concentration ( $L$ ) as  $L_{out} = 0.5L$ ;  $S_L$  is the mean area per lipid molecule:

$$S_L = f_{PC}S_{PC} + f_A S_A \tag{4}$$

here  $f_{PC}$ ,  $f_A$  are the mole fractions of PC and one of the three anionic phospholipids;  $S_{PC}$  is the mean area per PC molecule ( $0.65 \text{ nm}^2$ );  $S_A$  is the mean area per molecule of anionic phospholipid taken as  $0.65 \text{ nm}^2$  for PG or PS, and  $1.2 \text{ nm}^2$  for CL. The adsorption isotherm is described by the following equation [34]:

$$K_a(P - B) = \theta\gamma(\theta) \tag{5}$$

To reproduce the experimental FRET curves, the above adsorption model was combined with the model of energy

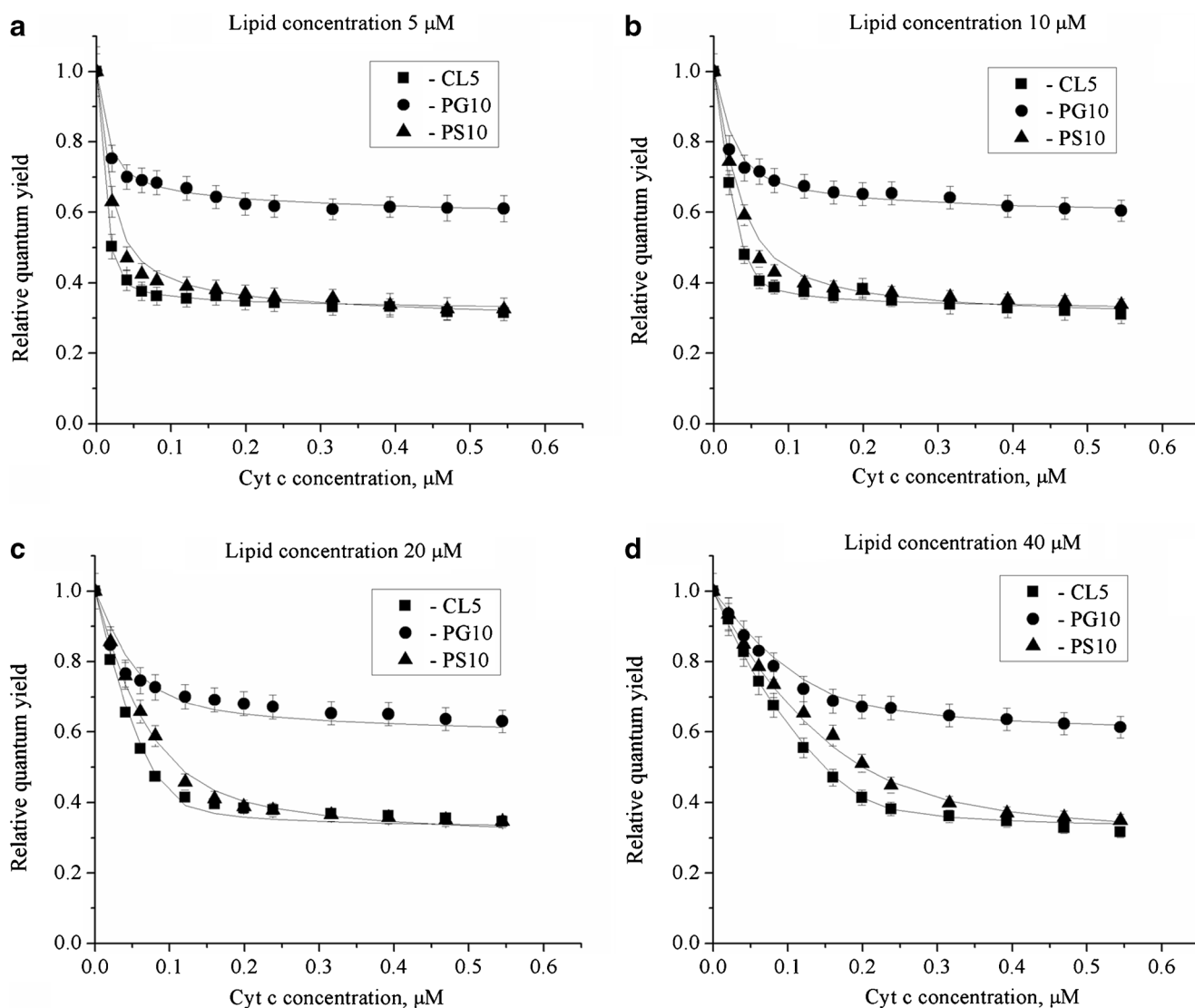


**Fig. 1** FRET profiles representing the relative quantum yield of AV-PC as a function of cytochrome *c* concentration for CL5, PS10 and PG10 liposomes. Lipid concentration was 5  $\mu\text{M}$  (a), 10  $\mu\text{M}$  (b),

20  $\mu\text{M}$  (c), 40  $\mu\text{M}$  (d). (b) and (c). Solid lines show theoretical curves calculated by numerical solution of Eqs. (3)–(11) with the model parameters presented in Table 1

transfer in two-dimensions, initially developed by Fung and Stryer [36] and extended in our previous studies to allow for the distance dependence of the orientation factor in the membrane systems and the possible heterogeneity of the donor or acceptor populations [37]. The examined cyt *c* – lipid systems were treated as containing one acceptor plane located at the distance  $d_c$  from the bilayer center, and two donor planes separated by a distance  $d_r$ . In this case, the relative quantum yield of the donor is given by:

$$Q_r = 0.5 \times \left( \int_0^\infty \exp(-\lambda) \exp \left[ -\frac{B}{S_L L_{out}} S_1(\lambda) \right] d\lambda + \int_0^\infty \exp(-\lambda) \exp \left[ -\frac{B}{S_L L_{out}} S_2(\lambda) \right] d\lambda \right) \quad (6)$$

$$S_1(\lambda) = \int_{d_c - 0.5d_r}^\infty \left[ 1 - \exp \left( -\lambda \kappa_1^2(R) \left( \frac{R'_o}{R} \right)^6 \right) \right] 2\pi R dR \quad (7)$$

$$S_2(\lambda) = \int_{d_c + 0.5d_r}^\infty \left[ 1 - \exp \left( -\lambda \kappa_2^2(R) \left( \frac{R'_o}{R} \right)^6 \right) \right] 2\pi R dR \quad (8)$$

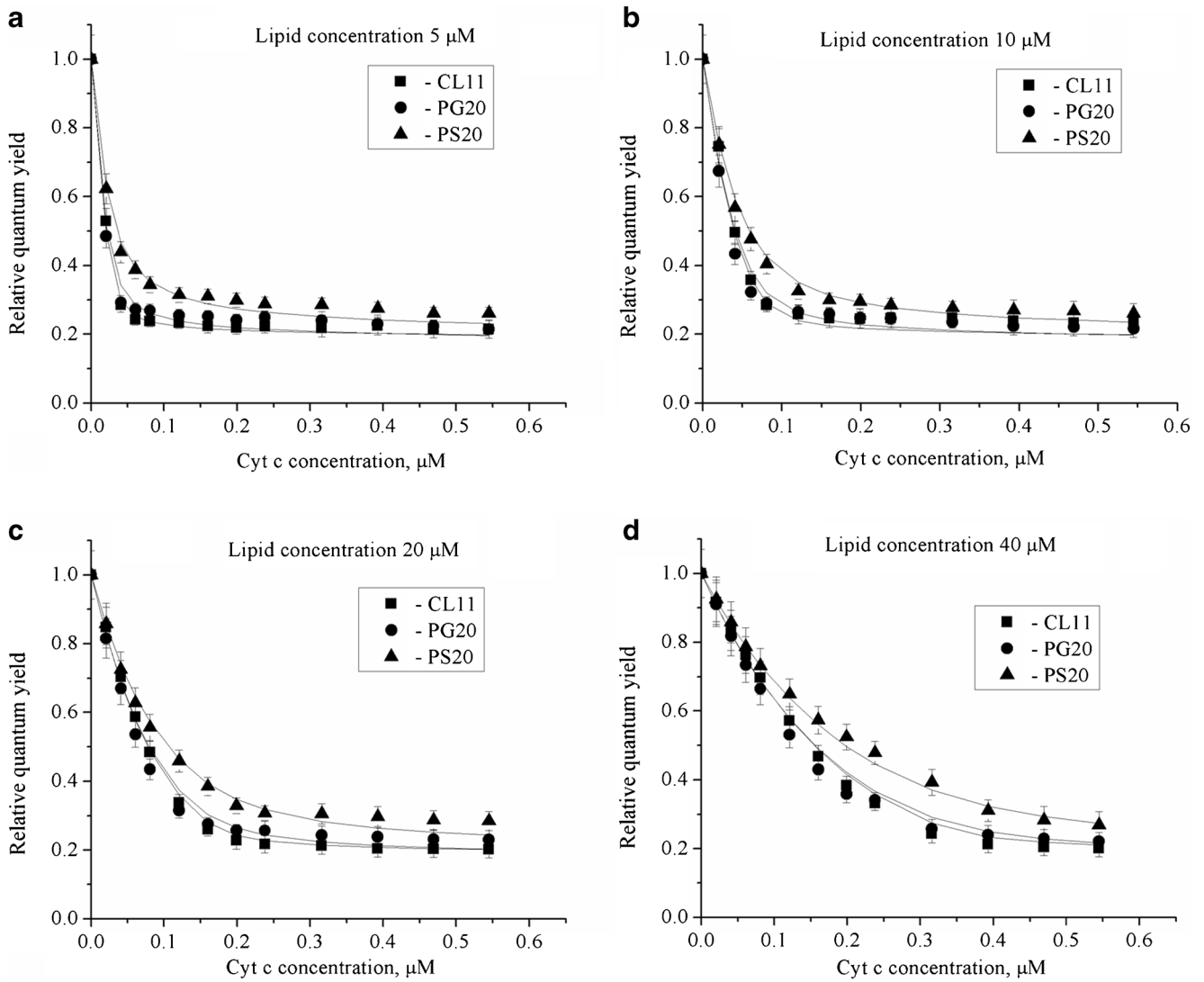


**Fig. 2** FRET profiles representing the relative quantum yield of AV-PC as a function of cytochrome *c* concentration for CL11, PS20, PG20 liposomes. Lipid concentration was 5 μM (a), 10 μM (b),

20 μM (c), 40 μM (d). (b) and (c). Solid lines show theoretical curves calculated by numerical solution of Eqs. (3)–(11) with the model parameters presented in Table 1

where  $R$  is the donor–acceptor separation,  $\lambda = t/\tau_d$ ;  $\tau_d$  is the lifetime of excited donor in the absence of acceptor. By representing the Förster radius as  $R_o = [\kappa^2(R)]^{1/6} \cdot R'_o$ , it follows that

$$R'_o = 979(n_r^{-4}Q_DJ)^{1/6} \quad J = \frac{\int_0^\infty F_D(\lambda)\epsilon_A(\lambda)\lambda^4 d\lambda}{\int_0^\infty F_D(\lambda)d\lambda} \quad (9)$$

here  $n_r$  is the refractive index of the medium ( $n_r = 1.37$ ),  $Q_D$  is the donor quantum yield (0.8),  $J$  is the overlap between the donor emission ( $F_D(\lambda)$ ) and acceptor absorption ( $\epsilon_A(\lambda)$ ) spectra [38]. Assuming that the donor emission and acceptor absorption transition moments are symmetrically distributed within the cones about certain axes  $D_x$  and  $A_x$ , the distance-dependent orientation factor is given by:

$$\kappa_{1,2}^2(R) = d_D d_A \left( 3 \left( \frac{d_c \mp 0.5d_t}{R} \right)^2 - 1 \right) + \frac{1 - d_D}{3} + \frac{1 - d_A}{3} + \left( \frac{d_c \mp 0.5d_t}{R} \right)^2 (d_D - 2d_D d_A + d_A) \quad (10)$$

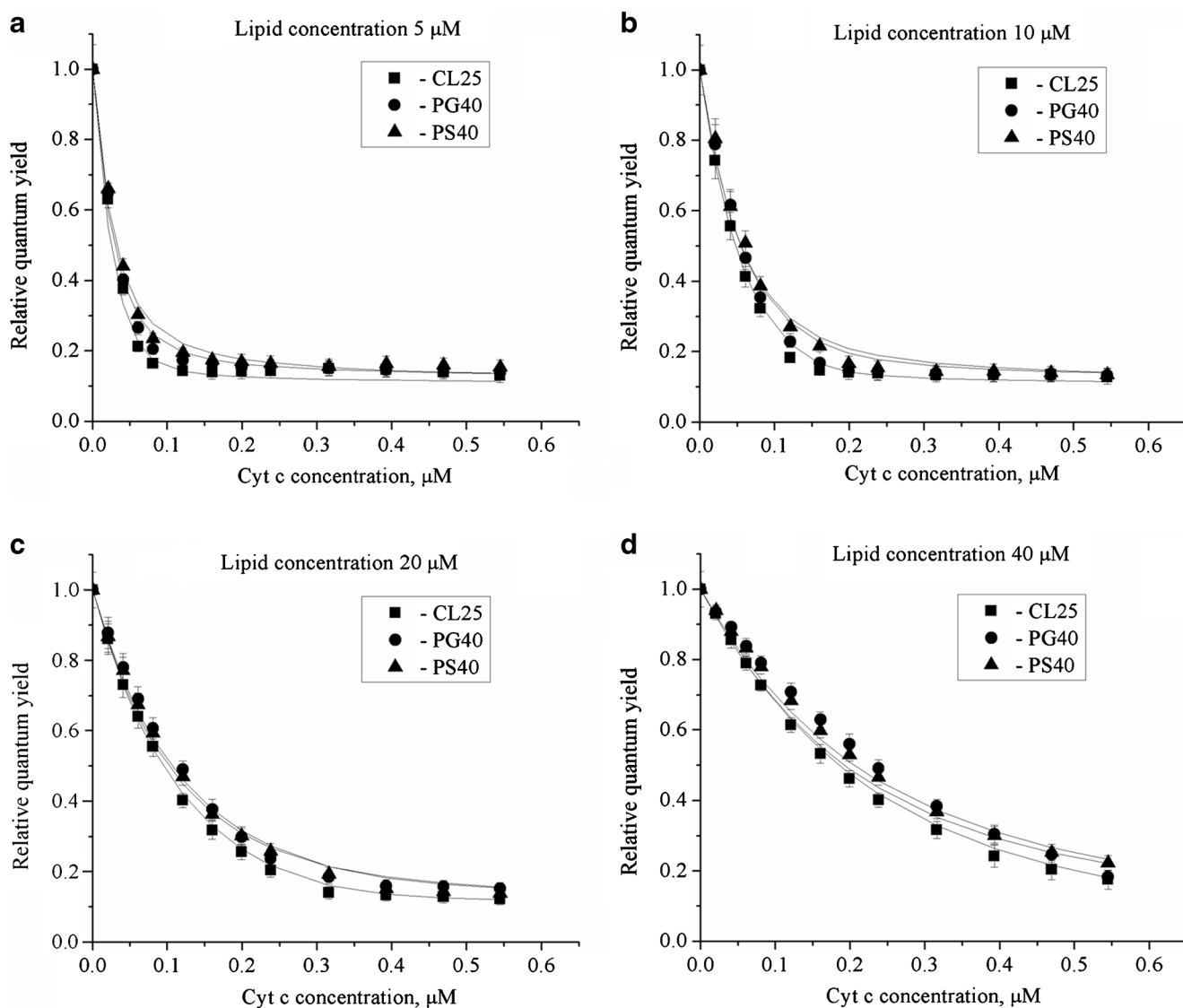


**Fig. 3** FRET profiles representing the relative quantum yield of AV-PC as a function of cytochrome *c* concentration for CL25, PS40, PG40 liposomes. Lipid concentration was 5 μM (a), 10 μM (b),

20 μM (c), 40 μM (d). (b) and (c). Solid lines show theoretical curves calculated by numerical solution of Eqs. (3)–(11) with the model parameters presented in Table 1

$$d_{D,A}^x = \langle d_{D,A}^x \rangle \left( \frac{3}{2} \cos^2 \alpha_{D,A} - \frac{1}{2} \right) \langle d_{D,A}^x \rangle = \left( \frac{3}{2} \cos^2 \psi_{D,A} - \frac{1}{2} \right) \quad (11)$$

where  $\psi_{D,A}$  are the cone half-angles,  $\alpha_{D,A}$  are the angles made by  $\mathbf{D}_x$  and  $\mathbf{A}_x$  with the bilayer normal  $\mathbf{N}$ . The axial depolarization factors  $\langle d_D^x \rangle$  and  $\langle d_A^x \rangle$  are related to the experimentally measurable steady-state ( $r$ ) and fundamental ( $r_0$ ) anisotropies of the donor and acceptor [39]:

$$d_{D,A}^x = \pm (r_{D,A}/r_{0D,A})^{1/2} \quad (12)$$

The donor depolarization factor  $d_D$  was calculated from Eq. 12 using the results of AV-PC anisotropy measurements. The  $r_D$  values appeared to fall in the range from 0.05 to 0.07.

The fundamental anisotropy of anthrylvinyl fluorophore was taken as 0.08 [30]. According to the linear dichroism data the transition moment of cyt *c* lies within the porphyrin plane [40], i.e.  $\psi_A = \pi/2$ . If cyt *c* adopts a certain specific orientation relative to the lipid-water interface, the porphyrin plane makes an angle  $\alpha_A$  with the bilayer surface. The results of FRET measurements presented here were analyzed within the two limiting assumptions: i)  $\alpha_A = 0$  (the porphyrin plane is parallel to the bilayer surface) and ii)  $\alpha_A = \pi/2$  (the porphyrin plane is perpendicular to the bilayer surface), thus allowing to estimate the upper and lower bounds of the  $d_c$  value.

Altogether, the set of the above equations was used to perform a global analysis of the FRET data arrays obtained upon varying the protein and lipid concentrations for a given



**Table 1** The binding and structural parameters derived for cyt *c* – lipid systems

System	Binding stoichiometry ( <i>n</i> )	Adsorption potential $J_A$ , in units of RT per anionic lipid	Adsorption potential $J_S$ , is units of RT per nm <sup>2</sup>	Heme distance from bilayer center $d_c$ , nm	<i>f</i>
CL <sub>5</sub>	48± <sup>2</sup>	7.6± <sup>0.3</sup>	0.6± <sup>0.03</sup>	2.4± <sup>0.1</sup>	7.4×10 <sup>-4</sup>
CL <sub>11</sub>	28± <sup>2</sup>	5.9± <sup>0.3</sup>	0.9± <sup>0.05</sup>	2.4± <sup>0.1</sup>	1.7×10 <sup>-3</sup>
CL <sub>25</sub>	14± <sup>3</sup>	5.2± <sup>0.3</sup>	1.6± <sup>0.09</sup>	2.7± <sup>0.2</sup>	1.9×10 <sup>-3</sup>
PS <sub>10</sub>	28± <sup>2</sup>	5.1± <sup>0.2</sup>	0.8± <sup>0.03</sup>	3.1± <sup>0.1</sup>	1.2×10 <sup>-3</sup>
PS <sub>20</sub>	18± <sup>2</sup>	4.0± <sup>0.2</sup>	1.2± <sup>0.06</sup>	3.2± <sup>0.1</sup>	1.3×10 <sup>-3</sup>
PS <sub>40</sub>	10± <sup>2</sup>	3.6± <sup>0.3</sup>	2.2± <sup>0.18</sup>	3.2± <sup>0.3</sup>	2.8×10 <sup>-3</sup>
PG <sub>10</sub>	50± <sup>6</sup>	2.9± <sup>0.4</sup>	0.4± <sup>0.06</sup>	4.0± <sup>0.4</sup>	3.5×10 <sup>-3</sup>
PG <sub>20</sub>	24± <sup>4</sup>	3.4± <sup>0.5</sup>	1.0± <sup>0.15</sup>	2.7± <sup>0.4</sup>	3.9×10 <sup>-3</sup>
PG <sub>40</sub>	10± <sup>2</sup>	3.9± <sup>0.5</sup>	2.4± <sup>0.31</sup>	3.4± <sup>0.3</sup>	3.7×10 <sup>-3</sup>

cyt *c* – lipid system. The numerical solution of these equations yielded the set of parameters { $K_a, n, d_c$ } providing the best agreement between experiment and theory (Table 1). The data fitting procedure was based on the minimization of the function:

$$f = \frac{1}{N} \sum_{i=1}^N (Q_{ri}^e - Q_{ri}^t)^2 \tag{13}$$

where *N* is the total number of the experimental points involved in the global analysis (*N*=64),  $Q_r^e$  is the experimental  $Q_r$  value,  $Q_r^t$  is the relative quantum yield calculated by the numerical integration of Eqs. (3)–(8).

To compare the binding characteristics of cyt *c* for the systems differing in the chemical nature of the anionic phospholipid headgroup, the recovered association constants were transformed into the adsorption potentials reflecting the variations in both quantities,  $K_a$  and *n*. These quantities

were expressed in the units of RT per nm<sup>2</sup> ( $J_S$ ) or per anionic lipid ( $J_A$ ):

$$J_S = \frac{\ln K_a}{nS_L}; J_A = \frac{\ln K_a}{nf_A} \tag{14}$$

As seen in Fig. 4, the adsorption potential calculated per unit area increases with increasing the surface electrostatic potential for a given type of anionic lipid, pointing to the prevailing role of electrostatic interactions in the cyt *c* - lipid binding. At the same time, the  $J_A$  values decrease in the rows: {CL<sub>5</sub>>PS<sub>10</sub>>PG<sub>10</sub>}, {CL<sub>11</sub>>PS<sub>20</sub>>PG<sub>20</sub>}, {CL<sub>25</sub>>PG<sub>40</sub>>PS<sub>40</sub>}, clearly showing the preference of cyt *c* for CL. It is worth noting at this point that our findings are in harmony with those of earlier studies [41–43]. More specifically, the affinity of cyt *c* for anionic phospholipids assessed by the surface plasmon resonance was found to decrease in the row: CL>PS>PC [43]. The solid-state <sup>31</sup>P NMR studies of cyt *c* interactions with lipid CL, PS and PG bilayers showed that regardless the main driving force of

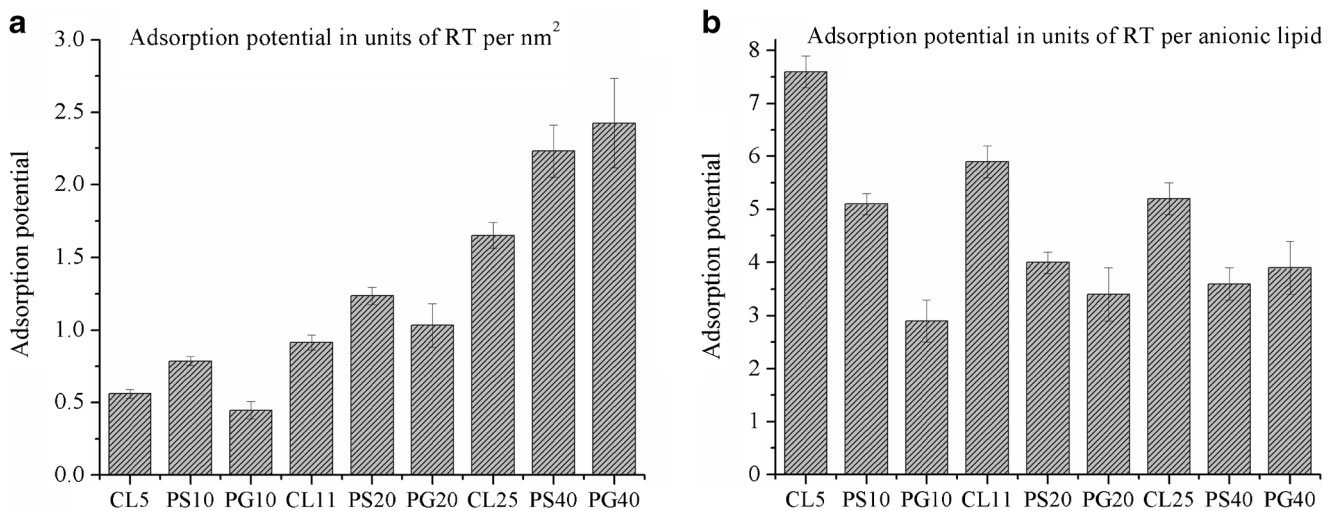


**Fig. 4** Adsorption potentials of cytochrome *c* binding to different types of liposomes expressed in units of RT per nm<sup>2</sup> (a) and in units of RT per anionic lipid (b)

all these interactions is electrostatic in nature, the structural alterations of the bound protein are lipid dependent [18, 41]. PS and CL were found to produce significant destabilization of cyt *c* structure, while in complexes with PG the protein retains a native-like conformation [41]. According to our FRET results, PG displays a binding behavior distinct from that of CL or PS, as most clearly seen in Fig. 1, showing the FRET curves measured at the lowest content of anionic lipid when the extent of protein binding was far from being complete. Interestingly, the resemblance between CL and PS in their effect on the structural state of cyt *c* was established in the early Raman [44, 45] and <sup>31</sup>P NMR [18] studies. The two different conformational states of cyt *c* adsorbed on the negatively charged surfaces have been identified – the native-like state I and state II, with the opened heme crevice. The equilibrium between these two states was supposed to be governed by the electrostatic interactions between lysine residues located around the heme crevice and the lipid phosphate groups. It was found that CL and PS promote the conformational equilibrium over the same temperature interval, while PG turned out to be less efficient in this respect, suggesting that cyt *c* conformation in complexes with PG is close to native [18]. A thorough recent work of Pandiscia & Schweitzer-Stenner provides evidence for an equilibrium between partially unfolded and native-like conformers of cyt *c* adsorbed on CL-containing bilayers, one of which forms electrostatic contacts with CL headgroups while the other one associates with lipids either via hydrogen bonding or hydrophobic interactions [26].

Along with the binding characteristics, the quantification of the presented experimental data in terms of the combined adsorption-FRET model yielded the structural parameter of the examined systems - the heme distance from the membrane midplane. The upper meaningful limit of this parameter, corresponding to a superficial location of cyt *c*, can be estimated as  $d_c^{\max} = 0.5d_m + r_{\text{cyt}} + r_t \sim 4.7$  nm, where  $d_m$  is the lipid bilayer width (4.6 nm),  $r_t$  is the displacement of heme group off the molecule center (*ca.* 0.7 nm). As seen from Table 1, in all CL-containing membranes the heme group is located closer to the membrane midplane, at the distance  $\sim 2.4$ – $2.7$  nm, while in the other liposomal membranes the heme resides at the greater distance from the bilayer center. Thus, cyt *c* - CL complexation is distinguished by the deeper membrane penetration of the protein compared to PS- and PG-containing systems. To interpret this particular behavior of CL we must consider some specific properties of this phospholipid, one of which consists in the formation of non-bilayer structures such as hexagonal ( $H_{II}$ ) phase [28]. This process involves gathering of CL molecules in the regions with negative curvature, i.e. hexagonal cylinders around cyt *c* and displacement of PC molecules from the protein vicinity. Vladimirov et al. have defined the hexagonal state of cyt *c* - CL complex as a spherical nanoparticle

with a diameter of  $\sim 11$  nm, where the protein is completely covered by the headgroups of 35–40 CL molecules [46]. In any case, the minimum separation between the heme moiety and AV group attached to methyl terminus of PC acyl chain would be greater than 4 nm, that is hard to reconcile with our  $d_c$  estimates.

Another specific property of CL is associated with its ability to adopt an extended conformation in which one [22, 23] or two [21] acyl chains protrude out of a membrane entering the hydrophobic cavity of cyt *c*. This type of protein-lipid interactions is specific for CL and is governed by its tendency to minimize the bending stress created by a high negative curvature. Notably, the ability of CL to adopt both the above configurations, extended anchorage and  $H_{II}$ , is supposed to originate from its conical shape inducing a negative curvature strain in the lipid bilayer [47]. A mechanistic model for the extended lipid anchorage proposed by Kalanxhi and Wallace [22] assumes that ionic contacts between phosphate group and Lys<sub>72</sub>, Lys<sub>73</sub> anchor CL in cyt *c* hydrophobic channel lined with the residues Tyr<sub>67</sub> - Pro<sub>71</sub> and Phe<sub>82</sub> - Ile<sub>85</sub>. Later, Sinibaldi et al. put forward the idea that this channel, together with the nonpolar pocket close to Asn<sub>52</sub> can simultaneously accommodate two of four hydrocarbon chains of CL [21]. Regardless of the exact mode of cyt *c* - CL complexation, the  $d_c$  values  $\sim 2.4$ – $2.7$  nm imply that the center of heme moiety is located in the aqueous phase close to the surface of PC/CL bilayers. On the other hand, in the native fold of cyt *c* the heme is separated from the surface of the protein molecule on average by 1.7 nm. If one assumes that CL-bound cyt *c* possesses native-like structure, the interfacial position of the heme group is consistent with the membrane embedment of the protein up to the level of terminal groups of hydrocarbon chains. However, this seems unlikely given the strongly basic nature of cyt *c*. Alternatively, our findings provide indirect arguments in favor of substantial reorganization of the protein structure accompanied by the exposure of nonpolar residues and the changes in the heme environment, that are in line with increasing evidence for CL-induced unfolding of cyt *c* [24–26]. In comparison with CL, PS and PG seem to provoke less pronounced destabilization of the protein molecule, resulting in the shallower location of cyt *c* relative to the lipid-water interface.

## Conclusions

Cumulatively, the measurements of the Förster resonance energy transfer between anthrylvinyl-labeled phosphatidylcholine as a donor and heme group as an acceptor revealed the differences in cytochrome *c* interactions with PC/CL, PC/PS and PC/PG lipid bilayers. The global analysis of the FRET data obtained at varying the molar fraction of anionic phospholipid, protein and lipid concentrations was



performed in terms of the SPT adsorption model combined with the model of energy transfer in two-dimensional systems. The main advantages of the employed theoretical approach are: (i) allowance for the area-excluding interactions between the adsorbed protein molecules and (ii) taking into account the distance dependence of the orientation factor in the membrane systems. The differences between CL on the one hand, and PS/PG on the other hand were quantitatively expressed in terms of the following parameters: the number of lipids per bound protein at saturation; adsorption potential and position of heme group relative to the lipid-water interface. The specificity of cyt *c* for CL is displayed in the higher adsorption potential per anionic lipid and deeper penetration of the protein in the lipid bilayer. The revealed specific features of cyt *c* – CL interactions may have important biological implications as a means of modulating the electron-transfer and apoptotic functions of this protein.

**Acknowledgements** This work was supported by the grant No 0116U000937 for Young Scientists from the Ministry of Education Science and of Ukraine.

## References

- Selvin PR (2000) The renaissance of fluorescence resonance energy transfer. *Nature Struct Biol* 7:730–734
- Sahoo H (2011) Förster resonance energy transfer—a spectroscopic nanoruler: principle and applications. *J Photochem Photobiol C* 12:20–30
- Ma L, Yang F, Zheng J (2014) Application of fluorescence resonance energy transfer in protein studies. *J Mol Struct* 1077:87–100
- Rowland CE, Delehanty JB, Dwyer CL, Medintz IL (2017) Growing applications for bioassembled Förster resonance energy transfer cascades. *Mater Today* 20:131–141
- Loura L, Prieto M (2011) FRET in membrane biophysics: an overview. *Frontiers Physiol* 92:1–11
- Corbalan-Garcia S, Sanchez-Carrillo S, Garcia-Garcia J, Gomez-Fernandez JC (2003) Characterization of the membrane binding mode of the C2 domain of PKC $\epsilon$ . *BioChemistry* 42:11661–11668
- Nazarov PV, Koehorst RB, Vos WL, Apanasovich VV, Hemminga MA (2006) FRET study of membrane proteins: simulation-based fitting for analysis of membrane protein embedment and association. *Biophys J* 91:454–466
- Silvius JR, Nabi IR (2006) Fluorescence-quenching and resonance energy transfer studies of lipid microdomains in model and biological membranes. *Mol Membr Biol* 23:5–16
- Calleja V, Ameer-Beg SM, Vojnovic B, Woscholski R, Downward J, Larijani B (2003) Monitoring conformational changes of proteins in cells by fluorescence lifetime imaging microscopy. *Biochem J* 372:33–40
- Chigaev A, Buranda T, Dwyer DC, Prossnitz ER, Sklar LA (2003) FRET detection of cellular  $\alpha_4$ -integrin conformational activation. *Biophys J* 85:3951–3962
- Yano Y, Takemoto T, Kobayashi S, Yasui H, Sakurai H, Ohashi W, Niwa M, Futaki S, Sugiura Y, Matsuzaki K (2002) Topological stability and self-association of a completely hydrophobic model transmembrane helix in lipid bilayers. *BioChemistry* 41:3073–3080
- You M, Li E, Wimley WC, Hristova K (2005) Förster resonance energy transfer in liposomes: measurements of transmembrane helix dimerization in the native bilayer environment. *Anal Biochem* 340:154–164
- Domanov Y, Gorbenko G, Molotkovsky J (2004) Global analysis of steady-state energy transfer measurements in membranes: resolution of structural and binding parameters. *J Fluoresc* 14:49–55
- Cusanovich MA, Hazzard JT, Meyer TE, Tollin G (1989) Electron transfer mechanisms in heme proteins. *J Macromol Sci Chem* A26:433–443
- Diaz-Moreno I, Garcia-Heredia JM, Diaz-Quitana A, De la Rosa MA (2011) Cytochrome *c* signalosome in mitochondria. *Eur Biophys J* 40:1301–1315
- Goodsell DS (2004) The molecular perspective: cytochrome *c* and apoptosis. *The Oncologist* 9:226–227
- Lewis RNA, McElhaney RN (2009) The physicochemical properties of cardiolipin bilayers and cardiolipin-containing lipid membranes. *Biochim Biophys Acta* 1788:2069–2079
- Pinheiro TJT (1994) The interaction of horse heart cytochrome *c* with phospholipid bilayers. Structural dynamic effects *Biochimie* 76:489–500
- Nantes IL, Zucchi MR, Nascimento OR, Faljoni-Alario A (2001) Effect of heme iron valence state on the conformation of cytochrome *c* and its association with membrane interfaces. *J Biol Chem* 276:153–158
- Sinibaldi F, Milazzo L, Howes BD, Piro MC, Fiorucci L, Polticelli F, Ascenzi P, Coletta M, Smulevich G, Santucci R (2017) The key role played by charge in the interaction of cytochrome *c* with cardiolipin. *J Biol Inorg Chem* 22:19–29
- Sinibaldi F, Howes BD, Droghetti E, Polticelli F, Piro MC, Di Pierro D, Fiorucci L, Coletta M, Smulevich G, Santucci R (2013) Role of lysines in cytochrome *c*–cardiolipin interaction. *Biochemistry* 52:4578–4588
- Kalanhni E, Wallace CJA (2007) Cytochrome *c* impaled: investigation of the extended lipid anchorage of a soluble protein to mitochondrial membrane models. *Biochem J* 407:179–187
- Tuominen EKJ, Wallace CJA, Kinnunen PKJ (2002) Phospholipid-cytochrome *c* interaction. Evidence for the extended lipid anchorage. *J Biol Chem* 277:8822–8826
- Hanske J, Toffey JR, Morenz AM, Bonilla AJ, Schiavoni KH, Pletneva EV (2012) Conformational properties of cardiolipin-bound cytochrome *c*. *Proc Natl Acad Sci USA* 109:125–130
- Muenzner J, Pletneva E (2014) Structural transformations of cytochrome *c* upon interaction with cardiolipin. *Chem Phys Lipids* 179:57–63
- Pandiscia LA, Schweitzer-Stenner R (2015) Coexistence of native-like and non-native partially unfolded ferricytochrome *c* on the surface of cardiolipin-containing liposomes. *J Phys Chem B* 119:1334–1349
- Brown L, Wuthrich K (1977) NMR and ESR studies of the interactions of cytochrome *c* with mixed cardiolipin-phosphatidylcholine vesicles. *Biochim Biophys Acta* 468:389–410
- De Kruijff B, Cullis PR (1980) Cytochrome *c* specifically induces non-bilayer structures in cardiolipin-containing model membranes. *Biochim Biophys Acta* 602:477–490
- Bergstrom CL, Beales PA, Lv Y, Vanderlick TK, Groves JT (2013) Cytochrome *c* causes pore formation in cardiolipin-containing membranes. *Proc Natl Acad Sci USA* 110:6269–6274
- Bergelson L, Molotkovsky J, Manevich Y (1985) Lipid-specific probes in studies of biological membranes. *Chem Phys Lipids* 37:165–195
- Molotkovsky J, Smirnova M, Karyukhina M, Bergelson L (1989) Synthesis of anthrylvinyl phospholipids probes. *Bioorg Khim* 15:377–380
- Bulychev AA, Verchoturov VN, Gulaev BA (1988) Current methods of biophysical studies. *Vyschaya Shkola, Moscow*

33. Malyshka D, Pandiscia LA, Schweitzer-Stenner R (2014) Cardiolipin containing liposomes are fully ionized at physiological pH. An FT-IR study of phosphate group ionization. *Vib Spectrosc* 75:86–92
34. Chatelier R, Minton AP (1996) Adsorption of globular proteins on locally planar surfaces: models for the effect of excluded surface area and aggregation of adsorbed protein on adsorption equilibria. *Biophys J* 71:2367–2374
35. Minton AP (1999) Adsorption of globular proteins on locally planar surfaces. II. Models for the effect of multiple adsorbate conformations on adsorption equilibria and kinetics. *Biophys J* 76:176–187
36. Fung BK, Stryer L (1978) Surface density determination in membranes by fluorescence energy transfer. *Biochemistry* 17:5241–5248
37. Gorbenko GP, Ioffe VM, Molotkovsky JG, Kinnunen PKJ (2008) Resonance energy transfer study of lysozyme-lipid interactions. *Biochim Biophys Acta* 1778:1213–1221
38. Lakowicz JR (2006) *Principles of fluorescent spectroscopy*. Springer, New York
39. Dale R, Eisinger J, Blumberg W (1979) The orientational freedom of molecular probes. The orientation factor in intramolecular energy transfer. *Biophys J* 26:161–194
40. Eaton WA, Hochstrasser RM (1967) Electronic spectrum of single crystals of ferricytochrome *c*. *J Chem Phys* 46:2533–2538
41. Pinheiro TJJ, Watts A (1994) Lipid specificity in the interaction of cytochrome *c* with anionic phospholipid bilayers revealed by solid-state  $^{31}\text{P}$  NMR. *Biochemistry* 33:2451–2458
42. Spooner PJR, Watts A (1991) Reversible unfolding of cytochrome *c* upon interaction with cardiolipin bilayers. 2. Evidence from phosphorus-31 NMR measurements. *Biochemistry* 30:3880–3885
43. Stepanov G, Gnedenko O, Mol'nar A, Ivanov A, Vladimirov Y, Osipov A (2009) Evaluation of cytochrome *c* affinity to anionic phospholipids by means of surface plasmon resonance. *FEBS Lett* 583:97–100
44. Hildebrandt P, Heimburg T, Marsh D (1990) Quantitative conformational analysis of cytochrome *c* bound to phospholipid vesicles studied by resonance Raman spectroscopy. *Eur Biophys J* 18:193–201
45. Heimburg T, Hildebrandt P, Marsh D (1991) Cytochrome *c*-lipid interactions studied by resonance Raman and  $^{31}\text{P}$  NMR spectroscopy. Correlation between the conformational changes of the protein and lipid bilayer. *Biochemistry* 30:9084–9089
46. Vladimirov YA, Nol' YT, Volkov VV (2011) Protein-lipid nanoparticles that determine whether cells will live or die. *Crystallogr Rep* 56:553–559
47. Cullis PR, de Kruijff B (1979) Lipid polymorphism and the functional roles of lipids in biological membranes. *Biochim Biophys Acta* 559:399–420